APPLIED PHYSICS LETTERS **90**, 262109 (2007)

Defect generation at the Si–SiO_2 interface following corona charging

Hao Jin,[a)] K. J. Weber, N. C. Dang, and W. E. Jellett
Centre for Sustainable Energy Systems, Faculty of Engineering and Information Technology, The Australian National University, Canberra ACT 0200, Australia

(Received 11 April 2007; accepted 25 May 2007; published online 28 June 2007)

A combination of capacitance-voltage and lifetime decay measurements is used to show that corona biasing of silicon oxidized samples results in the generation of additional interface defects and an increase in surface recombination. The onset of interface degradation occurs at relatively low electric fields, estimated to be less than $\sim +/-1.2$ MV/cm. The majority of the defects generated by corona biasing can be removed by a short annealing at 400 °C. The results are consistent with the hypothesis that atomic hydrogen is chiefly responsible for the observed degradation. Corona biasing, even at low electric fields, cannot be relied on as a noninvasive characterization tool. © *2007 American Institute of Physics*. [DOI: 10.1063/1.2749867]

The deposition of corona charges is extensively used for device reliability characterization[1,2] as well as for fundamental studies on many types of devices and structures, including solar cells.[3,4] Corona charging in air is considered to gently deposit ionic species—$(H_2O)_nH^+$ or carbonate ions (CO_3^-)—onto the dielectric layer such as silicon dioxide (SiO_2), covering the silicon (Si) substrate. The presence of these external charges, as an alternative to external bias,[5] creates an electrical field and influences the Si surface band bending. Corona charging is a particularly attractive technique because it requires little sample preparation and is generally considered noninvasive. For photovoltaics research, in particular, an additional advantage is the fact that the optical properties of the sample under test are not altered by the application of charge. The ability to vary the Si surface band bending through the application of charge is crucial for photovoltaics research, since charge is always present in the dielectric films used as surface passivation layers and antireflection coatings, and since this charge is well known to have a dramatic influence on surface carrier recombination and therefore solar cell performance.

It has been known for some time, from electron spin resonance (ESR) studies using high field corona bias, that high oxide field corona biasing can generate large densities of Si–SiO_2 interface and oxide paramagnetic centers.[6–8] However it has generally been assumed that, provided such high fields are avoided, corona biasing is a noninvasive technique which merely leads to a variation in the surface charge density. Recent publications by Stesmans and Afanas'ev[7,8] have suggested that this assumption is not valid, and that corona biasing is an inherently unreliable technique that can lead to significant interface modification. Dautrich *et al.*[6] have disagreed with these conclusions and maintain that, at low electric fields, corona biasing can safely be used without danger of interface modification.

The above mentioned studies have used ESR as the chief characterization tool, in order to allow identification of the nature of (paramagnetic) interface defects, as well as their density. In this work, we use minority carrier lifetime and capacitance-voltage (*C-V*) measurements to study the Si–SiO_2 interface. In addition to providing information on the parameters of chief interest for photovoltaics, namely, the effective lifetime and the surface recombination velocity, these measurements have the further advantage of not being restricted to ESR-active defects. As pointed out by Stesmans and Afanas'ev, the disadvantage of these electrical techniques is that they provide little information on the nature of the defects involved, so that the various characterization tools must be viewed as complementary.

Float zoned, (100), ($>100\ \Omega$ cm) *p*-type, 500 μm thick wafers were used for effective carrier lifetime measurements. Czochralski, (100), 10–23Ω cm *p*-type wafers were used for *C-V* measurements. After RCA (Radio Corporation of America) cleaning,[9] all samples received a 50 nm thick thermal oxide grown at 1000 °C in dry oxygen followed by a 30 min *in situ* annealing in nitrogen (N_2) at the same temperature. The *in situ* annealing further improves the Si interface properties.[10] All samples were annealed in forming gas [5% hydrogen (H_2) in 95% argon (Ar), FGA] at 400 °C for 30 min. ~5 nm aluminum (Al) was deposited on both sides of some samples for lifetime measurements in order to form symmetric metal-oxide-semiconductor (MOS) structures. These samples were then used for measurements of the lifetime as a function of applied voltage (no corona charging). Details of the process can be found elsewhere.[11] The oxide was removed from one side for the *C-V* samples.

Corona charging was carried out with a conventional setup[2] by applying voltage of +/−10 kV to a steel needle about 5 cm above the samples (current drawn of $\sim 2\ \mu A/cm^2$). On samples for lifetime measurements, corona charging was carried out on both sides, sequentially, for equal amounts of time. Note that these samples did not have an Al layer on the oxide. On samples for *C-V* measurements, corona charging was only done on the oxidized surface. Following corona charging, some samples received a RCA clean, followed by a rapid thermal annealing (RTA) in N_2 at 400 °C for 30 s and a subsequent FGA at 400 °C for 30 min.

Lifetime measurements were carried out using the inductively coupled photoconductivity decay technique.[12,13] The effective lifetime is determined from the rate of decay of the wafer photoconductivity following the application of a light pulse. In high injection, the measured instantaneous decay time τ_{inst} is[13]

a)Electronic mail: hao.jin@anu.edu.au

 © 2007 American Institute of Physics
Downloaded 13 Mar 2008 to 150.203.45.168. Redistribution subject to AIP license or copyright; see http://apl.aip.org/apl/copyright.jsp

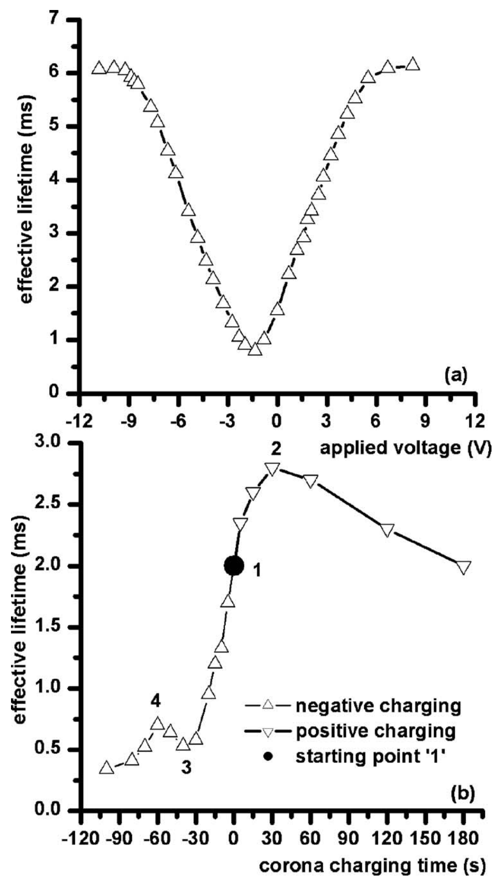

FIG. 1. Effective lifetime (at an injection level of 4×10^{15} cm^{-3}) for oxidized Si samples after as a function of (a) applied bias voltage on a MOS structure and (b) corona charging time.

$$1/\tau_{\text{inst}} = 1/\tau_{\text{hli}} + 2S_{\text{eff}}/W, \tag{1}$$

where τ_{hli} is the high level injection lifetime of the wafer bulk, W is the wafer thickness, and S_{eff} is the effective surface recombination velocity, defined by

$$S_{\text{eff}} = U/n, \tag{2}$$

where U is the surface recombination rate per unit area and n is the excess carrier density in the wafer bulk. Measurements were carried out at an injection level of 4×10^{15} cm^{-3}.

Prior to *C-V* measurements, ~80 nm Al was deposited with an area of around 4.7×10^{-3} cm^2 through a shadow mask on the oxide to form a MOS structure. High frequency *C-V* measurements were carried out at 1 MHz and quasi-static *C-V* measurements were carried out with a sweep rate of 50 mV/s. The Castagne and Vapaille[14] method was used to determine the defect distribution.

Figure 1 shows the variation of the effective lifetime with applied bias voltage (a) and with corona charging time (b). Under the influence of an applied voltage, the characteristic "U" shape is observed, with a minimum for depletion conditions at the surface, and saturating to maximum values for accumulation (at large negative voltages) and deep inversion (at large positive voltages) conditions. The minimum occurs at a small negative applied bias due to the $Al-SiO_2-Si$ work function difference and a low density of positive charge at the $Si-SiO_2$ interface of the as grown oxide.[11]

Two samples, with nearly identical initial lifetimes, were used for the corona charging curves—one for the cumulative deposition of positive charge and one for the cumulative deposition of negative charge. With increasing positive charging time, the curve initially appears similar to the applied voltage–lifetime curve, with a sharp increase in the effective lifetime. However, instead of saturating, the lifetime starts to decrease again at point 2 on the curve. With negative charging, the curve also initially is qualitatively similar to the applied voltage–lifetime curve, with a minimum in the lifetime after a relatively short exposure to negative charge (point 3). After this point, the lifetime rises and soon afterwards declines again (at point 4).

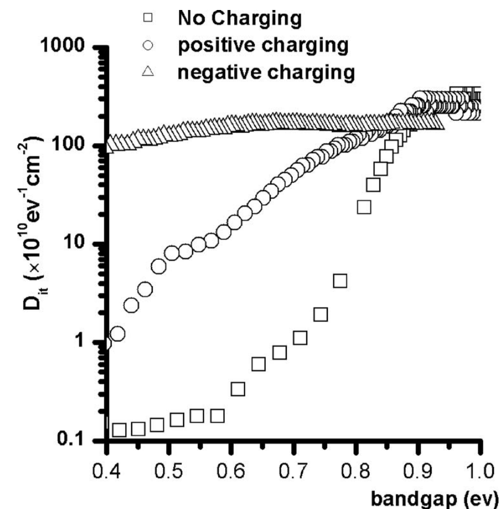

FIG. 2. Comparison of D_{it} distribution within the Si forbidden bandgap. "-○-:" as oxidized sample; "-△-:" after 26 min positive corona charging, and "-□-:" after 26 min negative corona charging.

These results show that both positive and negative corona charging either introduce additional interface defects or activates previously deactivated (hydrogen passivated) defects. The points at which a clear decrease in the lifetime can be observed [points 2 and 4 in Fig. 1(b)] indicate the latest possible onset of the degradation of the surface properties. In reality the onset probably occurs earlier (for shorter charging times) but is masked by the effect of increasing (positive or negative) charge, which leads to a decrease in the surface minority carrier concentration and to an overall decrease in surface recombination. Comparing these points with the lifetime-voltage curve in Fig. 1(a), it can be concluded that the onset of degradation occurs at relatively low values of the electric field. Conservatively, we estimate the onset to be at less than ~+/−1.2 MV/cm or +/−6 V. In contrast, Dautrich *et al.*[6] found no evidence of degradation, using ESR measurements, for positive electric fields up to 4 MV/cm.

Figure 2 shows the defect density (D_{it}) distributions of an as oxidized Si sample and of samples following 26 min of positive or negative corona charging. Since *p*-type samples were used for the measurements, accurate information is obtained for the upper half of the band gap only. A substantial increase in D_{it} can be observed for the corona charged samples, with the increase being particularly dramatic for the negatively charged sample. The midgap D_{it} for the negatively charged sample is almost three orders of magnitude higher than for the as oxidized sample, while for the positively charged sample the difference is a factor of 40.

In order to investigate further the nature of the defects introduced by corona charging, the samples received a RTA for 30 s at 400 °C in dry N_2, and subsequently a FGA at

Downloaded 13 Mar 2008 to 150.203.45.168. Redistribution subject to AIP license or copyright; see http://apl.aip.org/apl/copyright.jsp

TABLE I. Comparison of midgap D_{it} of samples following various processing steps. Corona charging was carried out for 26 min per side.

		Midgap $D_{it}(\times 10^{10}\ \mathrm{eV^{-1}\ cm^{-2}})$
As oxidized		0.16
Corona charged	Positive	6.5
	Negative	146
Corona+RTA	Positive	1.6
	Negative	4.0
Corona+FGA	Positive	0.40
	Negative	0.47

400 °C for 30 min. Table I summarizes the effect of these treatments on midgap D_{it} values. The short RTA treatment results in a substantial reduction in defect density, particularly for the negatively charged sample. The FGA results in a further reduction of midgap D_{it}, but not to back to the value of the as oxidized sample.

Stesmans and Afanas'ev[7,8] observed at least five ESR-active defects following positive corona biasing, including the activation of (initially hydrogen passivated) Pb_0 and Pb_1 centres (but not the generation of additional Pb_x centers), and the generation of UL1 and E'_γ centers at relatively low concentrations of several $10^{10}\ \mathrm{cm}^{-3}$. The authors suggested that the observed activation and generation of defects were chiefly the result of the action of atomic or protonic hydrogen, generated by the corona discharge process, which is able to diffuse through the oxide and interacts with the interface.

Our results are broadly consistent with those of Stesmans and Afans'ev, and with the suggestion that atomic or protonic hydrogen is chiefly responsible for the interface degradation. The very high D_{it} values measured after negative corona charging are chiefly the result of non-ESR-active defects, since the majority of the defects are removed by a short RTA treatment (the density of ESR-active Pb_x centers would not be affected by such an annealing). Cartier *et al.*[15] have previously observed that atomic hydrogen exposure of oxidized Si samples at room temperature can cause partial depassivation of Pb_x centers and leads to the generation of a large density of additional defects which could not be detected by ESR. Our previous work[16] indicates that the majority of these atomic H generated defects can be removed by a subsequent short RTA at 400 °C. The results therefore support the conclusion that the corona damage is mainly due to atomic hydrogen.

The further reduction in defect density following a FGA treatment is attributed to a repassivation of Pb_x centers by molecular hydrogen. For the positively corona charged sample, the defect density following charging is much lower but the same trend with annealing is observed, with a reduction in D_{it} following both the RTA and FGA treatments. However, it is noteworthy that, for both positively and negatively corona charged samples, the defect density does not return to the "as oxidized" level even after the FGA treatment.

Perhaps most significant from a practical point of view is the observation that the onset of interface degradation in our samples occurs at a relatively low electric field, so that it is not possible to avoid degradation merely by avoiding high electric fields of the order to 7 MV/cm. The degradation at low electric fields cannot be attributed to Fowler-Nordheim electron injection. Instead, our observations are broadly consistent with the hypothesis that atomic or protonic H is the chief culprit (for both positive and negative corona biases) by partly depassivating Pb_x centers, as well as causing the generation of other defects.

The authors would like to thank Keith McIntosh, Andrew Thomson, and Luke Johnson for regular discussions. Support from the Australian Research Council for this work is acknowledged.

[1]W. L. Warren and P. M. Lenahan, Appl. Phys. Lett. **49**, 1296 (1986).
[2]Z. A. Weinberg, W. C. Johnson, and M. A. Lampert, J. Appl. Phys. **47**, 248 (1976).
[3]S. W. Glunz, D. Biro, S. Rein, and W. Warta, J. Appl. Phys. **86**, 683 (1999).
[4]A. G. A. J. Schmidt, Prog. Photovoltaics **6**, 259 (1998).
[5]R. B. M. Schoefthaler, R. Brendel, G. Langguth, and J. H. Werner, Proceedings of the First World Conference on Photovoltaic Energy Conversion (1994), p. 1509.
[6]M. S. Dautrich, P. M. Lenahan, A. Y. Kang, and J. F. Conley, Appl. Phys. Lett. **85**, 1844 (2004).
[7]A. Stesmans and V. V. Afanas'ev, Appl. Phys. Lett. **82**, 2835 (2003).
[8]A. Stesmans and V. V. Afanas'ev, Microelectron. Eng. **72**, 55 (2004).
[9]W. Kern and D. A. Puotinen, RCA Rev. **31**, 187 (1970).
[10]A. G. Aberle, Prog. Photovoltaics **8**, 473 (2000).
[11]W. E. Jellett and K. J. Weber, Appl. Phys. Lett. **90**, 042104 (2007).
[12]E. Yablonovitch and T. J. Gmitter, Solid-State Electron. **35**, 261 (1992).
[13]D. E. Kane and R. M. Swanson, Proceedings of the 18th IEEE Photovoltaic Specialists Conference (1985), p. 57.
[14]R. Castagne and A. Vapaille, Surf. Sci. **28**, 157 (1971).
[15]E. Cartier, J. H. Stathis, and D. A. Buchanan, Appl. Phys. Lett. **63**, 1510 (1993).
[16]H. Jin, K. J. Weber, and P. J. Smith, J. Electrochem. Soc. **154**, H430 (2007).

Downloaded 13 Mar 2008 to 150.203.45.168. Redistribution subject to AIP license or copyright; see http://apl.aip.org/apl/copyright.jsp